Temperature dependence of the elastic modulus of crystalline regions of polyoxymethylene*

Katsuhiko Nakamae†, Takashi Nishino, Yukio Shimizu and Katsuhiko Hata

Department of Industrial Chemistry, Faculty of Engineering, Kobe University, 1 Rokko-dai, Nada, Kobe 657, Japan

(Received 5 June 1989; revised 27 September 1989; accepted 6 October 1989)

The temperature dependence of the elastic modulus E_l of crystalline regions in the direction parallel to the chain axis of various polyoxymethylenes (POM) has been investigated by X-ray diffraction. An E_l value of 52 GPa is obtained for both hot-drawn (draw ratio $\lambda=14$ at 170°C) and annealed (170°C, 1 h) POM (specimen modulus $Y_l=27$ GPa) and drawn ($\lambda=5$ at 140°C) POM ($Y_l=6.4$ GPa) at room temperature, which agrees well with that previously reported. However, the E_l value of POM ($\lambda=34$ under dielectric heating, MISELA (microwave selective adsorption), $Y_l=60$ GPa) is 73 GPa at room temperature, which exceeds the Y_l of MISELA and is higher than the E_l value of hot-drawn and annealed POM. The E_l values of both hot-drawn and annealed POM and MISELA are in accord with each other and 85 GPa is obtained at −150°C, but the temperature dependences of E_l of these POM differ much from each other. With increasing temperature, the E_l value decreased and reached a plateau at 0°C for hot-drawn and annealed POM (52 GPa), but for MISELA E_l reached a plateau of 73 GPa at −60°C. Further, E_l values decreased at 100°C for both samples. The lattice spacing for the (0 0 9) plane of each POM also decreases with increasing temperature in the temperature range studied. The thermal expansion coefficients change discontinuously in the ranges 0 to 100°C for hot-drawn and annealed POM and −60 to 100°C for MISELA. These temperature ranges agree with that where the temperature dependence of E_l changed, that is, thermal molecular motion in the crystalline regions changed. Consequently, the mobility of a chain molecule, i.e. incoherent thermal vibration, differs from hot-drawn and annealed POM to MISELA, and this causes the difference in temperature dependence of E_l for the two kinds of POMs. Further, the discrepancy in the E_l values for these samples at room temperature is in fact not because of the inhomogeneous stress distribution but because of the difference in the mobility of chain molecules in the crystalline regions at room temperature.

(Keywords: crystal modulus; polyoxymethylene; temperature dependence; elastic modulus; mechanical property)

INTRODUCTION

The elastic moduli of polymer crystals give us information on the molecular conformation and intermolecular forces in the crystal lattice, and on the relation of these to mechanical properties of the polymers[1–7]. We have been engaged in measuring the elastic modulus E_l of crystalline regions of various polymers in the direction parallel to the chain axis by X-ray diffraction. Examinations of the data so far accumulated led us to success in relating the E_l value—viz. the extensivity and the deformation mechanism of a polymer molecule—to the molecular conformation in the crystal lattice. The values of E_l for polymers with a fully extended planar zigzag conformation, i.e. polyethylene (PE) and poly(vinyl alcohol) (PVA), are found to be 235 and 250 GPa, respectively[1–4]. The extension of a polymer chain with helical or contracted conformation in the crystal lattice involves simultaneous free rotation about the single bonds of the chain, in addition to the mechanisms for the fully extended structure. The force constant of internal rotation is smaller than those of bond stretching and bond angle bending. For this reason, E_l values for these polymers are small[1–4].

Polyoxymethylene (POM) is the first member of the polyether series and one of the most popular plastics. The POM molecule has a 9/5 helix in the crystalline regions and packs in a trigonal unit cell. The E_l value for POM was reported to be 53 GPa by X-ray diffraction, which is about one-fifth of those for PE and PVA[3].

Knowledge of the elastic modulus E_l of crystalline regions of polymers is of interest from another point of view, i.e. in connection with mechanical properties of polymers, because E_l gives us the maximum value for the specimen modulus of a polymer[6–8]. In recent years, much effort has been applied to obtaining molecular extension and alignment in solid polymers with the aim of exploiting the high-modulus and high-strength polymer[9]. So applications to POM have also been investigated by many workers[10–12]. It has been reported that high-modulus POM up to 40 GPa is produced by solid-state polymerization of trioxane[10], tensile drawing[11], hydrostatic extrusion[12], die drawing[13], pressurized drawing[14], etc. One out of many POM produced by tensile drawing under dielectric heating (microwave selective adsorption hot-drawing method; MISELA) gave the highest Young's modulus of 63 GPa at room temperature[15]. This value

* Studies on the temperature dependence of the elastic modulus of crystalline regions of polymers: 11

† To whom correspondence should be addressed

0032-3861/90/101909-10

exceeds the previously reported E_l value at room temperature. This phenomenon needs us to re-examine the E_l value of POM at room temperature.

Further, we have also investigated the temperature dependence of E_l for some polymers at high temperature and discussed this in terms of the thermal expansivity and stability of the crystalline regions of each polymer. In many cases, such as poly(butylene terephthalate)[16], isotactic polypropylene[17], poly(ethylene oxybenzoate)[18], PE[19], PVA[20], poly(*p*-phenylene terephthalamide)[21], polytetrafluoroethylene[22], nylon-6[23], polytetrahydrofuran[24], poly(ethylene terephthalate)[25] and poly(4-methyl-1-pentene)[26], the E_l value decreases above a certain temperature. Brew *et al.* also reported that the E_l value for POM increases with decreasing temperature and reaches 105 GPa at -165°C[27].

POM has wide practical usages in areas such as engineering plastics, etc., and is applicable in various environmental conditions. This suggests the need to clear up the relationships between Young's modulus, tensile strength and temperature.

In this paper, we report the reproducibility of the E_l value and its temperature dependence from -150°C to $+150$°C for various kinds of POM, including MISELA.

EXPERIMENTAL

Samples

Three different kinds of POM samples were used in this study.

Hot-drawn and annealed POM. Commercial-grade pellets (Du Pont, Delrin 100) were melt-spun at 220°C followed by rapid cooling into ice–water. Spun fibre was drawn to 14 times its original length at 170°C, and annealed at 170°C for 1 h at constant length.

Drawn POM. Compression-moulded film of Delrin 100 was quenched from the melt (220°C) into ice–water. Rectangular samples cut from this film were drawn five times at 140°C followed by rapid quenching.

MISELA. POM rod (Asahi Chemical Industry Co. Ltd, Tenac 5010) was drawn 34 times under a dielectric heater, which was kindly supplied by Dr Nakagawa and Dr Yamakawa, Ibaraki Electrical Communication Laboratory, Nippon Telegraph and Telephone Co[15]. In this way, it is expected that the non-crystalline regions and crystal defects are selectively heated more intensively by dielectric heating; therefore, the drawing stress acts effectively upon the disordered regions[15]. This results in an effective amorphous orientation.

Methods

Figure 1 shows the X-ray fibre photographs of each POM at room temperature. All specimens show high crystallinity and high degree of orientation of crystalline regions, and all reflections can be indexed with the trigonal unit cell.

The melting point T_m of the specimen was obtained as the peak melting temperature by using a differential scanning calorimeter (Daini Seikosha SSC-560S) at a heating rate of 10°C min^{-1} and sample weight of 5 mg. Heat of fusion ΔH was also obtained as the area of the melting peak. Values of T_m and ΔH were calibrated with indium.

The degree of crystallinity X_c was calculated by the following equation:

$$X_c = \Delta H / \Delta H_0 \quad (1)$$

where ΔH_0 is the equilibrium heat of fusion (59 cal g^{-1})[28].

The degree of crystal orientation Π was defined by:

$$\Pi = (180 - H^0)/180 \quad (2)$$

where H^0 is the half-width of the intensity distribution curve along the Debye–Scherrer ring of the (0 0 9) reflection of each POM.

The determination of crystallite size and lattice distortion of POM along the chain direction was performed by measuring meridional profiles of the (0 0 9) and (0 0 18) reflections. Observed integral widths of each reflection were corrected for both the Cu K_α doublet broadening (Jones' method)[29] and the instrumental broadening b according to the equation:

$$\beta^2 = B^2 - b^2 \quad (3)$$

where β is the pure integral width of the reflections. The integral width (δS) in reciprocal lattice space was given as follows:

$$(\delta S) = \beta \cos\theta / \lambda \quad (4)$$

where θ is the Bragg angle and λ is the wavelength of the X-ray.

POM shows only two meridional reflections (0 0 9) and (0 0 18) for Cu K_α radiation; the lattice distortion g_{II} was assumed to be paracrystalline type. Then δS can be expressed as so-called Hosemann's plot:

$$(\delta S)^2 = (1/D^2) + (\pi^4 g_{II}^4 m^4 / d^2) \quad (5)$$

where m is the order of reflections and d is the fibre

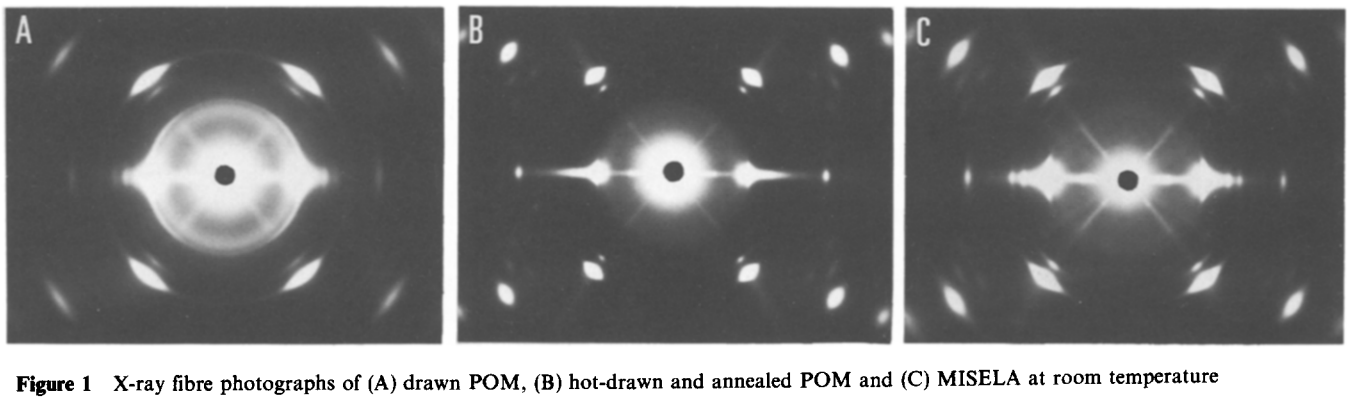

Figure 1 X-ray fibre photographs of (A) drawn POM, (B) hot-drawn and annealed POM and (C) MISELA at room temperature

identity period. Then crystallite size D and the paracrystalline distortion g_{II} in the direction parallel to the chain axis were obtained from the intercept and slope of the $(\delta S)^2$ *versus* m^4 plots[30].

The crystallite size $D_{(hk0)}$ of POM in the direction perpendicular to the chain axis was obtained from the (1 1 0) and (1 0 0) reflections using equation (4).

The stress–strain curve for the specimen was measured by a tensile tester (Shimazu, Autograph IS-100) at room temperature. The initial length of the specimen was 10 mm and the extension rate was 2 mm min^{-1}.

Measurement of the elastic modulus of crystalline regions

The unit cell of POM crystal used in this study is a trigonal system with $a=4.47$ Å and $c=17.39$ Å[8]. The lattice plane of POM used for the measurement of the elastic modulus E_l is meridional reflections, (0 0 9); 2θ for Cu K_α radiation is 47.03°.

The lattice extension under a constant load was measured by means of an X-ray diffractometer (Rigaku Denki RAD-B System) equipped with a stretching device. The strain ε in the crystalline regions was estimated by use of the relation:

$$\varepsilon=\Delta d/d_0 \qquad (6)$$

where d_0 denotes the initial lattice spacing and Δd is the change in lattice spacing induced by a constant stress. The determination of peak position was performed by eye and calibrated with aluminium powder. The experimental error in measuring the peak shift was evaluated ordinarily to be less than $\pm 1/100°$ in angle 2θ. This corresponds to 0.000 39 Å and therefore we can measure the strain within experimental error of $\pm 0.020\%$.

The stress σ in the crystalline regions was assumed to be equal to the stress applied to the sample. This assumption of a homogeneous stress distribution has been proven experimentally for PE, PVA, cellulose[1–4,19], poly(ethylene terephthalate)[25], poly(*p*-phenylene terephthalamide)[21], etc.

The elastic modulus E_l was calculated as:

$$E_l=\sigma/\varepsilon \qquad (7)$$

A more detailed description of the measurements was given in earlier papers[1–4].

E_l values at high and low temperature were measured by using heating (electric heater) and cooling (N_2 cooled gas) cells with a temperature controller on an X-ray diffractometer[16–26]. The temperature was detected with a thermocouple placed 5 mm from the sample, and it could be maintained within ± 1°C during the measurements.

RESULTS AND DISCUSSION

Characterization of various POMs

Table 1 shows some properties of the three kinds of POM used in this study. The melting point T_m, heat of fusion ΔH, crystallinity X_c and crystallite sizes both parallel D and perpendicular $D_{(hk0)}$ to the chain axis increase successively in the order of drawn POM, hot-drawn and annealed POM, and MISELA. Further, lattice constant c becomes longer and a becomes shorter. These differences of lattice constant (for example, it corresponds to $\Delta(2\theta)=0.288°$ for (0 0 9) reflection) are beyond the experimental error ($\pm 1/100°$), and the same was also confirmed with (0 0 18) reflection. Accordingly, molecular packing in the crystal lattice became better in the order described above. Specimen modulus Y_l of MISELA is 60 GPa, which exceeds the E_l value (53 GPa)[1–4] mentioned above, and compares with the Y_l values of drawn POM and hot-drawn and annealed POM. However, the degree of crystal orientation Π of MISELA is unexpectedly low despite the fact that draw ratio and Y_l are high for MISELA. This is also clear qualitatively from the X-ray photographs shown in *Figure 1*.

E_l of various POMs at room temperature

In order to examine the reproducibility of the E_l value of POM, we first measured the E_l value at room temperature.

Figure 2 shows the stress(σ)–strain(ε) curves for the (0 0 9) plane of hot-drawn and annealed POM and MISELA at 25°C. The lattice extensions were always reversible. From *Figure 2a*, the curve can be expressed with the two straight lines through zero, inflected at about 230 MPa or a lattice extension of 0.4%, below and above which the slopes of the curve changed. The initial slope gives us the E_l value of 52 GPa, and the elastic modulus E_l' in the upper stress region is 29 GPa. The f value, the

Table 1 Properties of three kinds of polyoxymethylene

	Drawn POM	Hot-drawn and annealed POM	MISELA
Melting point, T_m (°C)	181	184	186
Heat of fusion, ΔH (cal g^{-1})	38.4	49.7	56.0
Crystallinity (%)	65.1	84.2	95.0
Degree of orientation	0.946	0.975	0.971
Crystallite size			
Chain direction, D (Å)	101	161	209
Distortion, g_{II} (%)	0.66	0.59	0.62
(1 0 0) (Å)	74	102	184
(1 1 0) (Å)	88	111	163
Lattice constant			
a (Å)	4.54	4.51	4.45
c (Å)	17.29	17.38	17.39
Specimen modulus, Y_l (GPa)	6.4	27	60

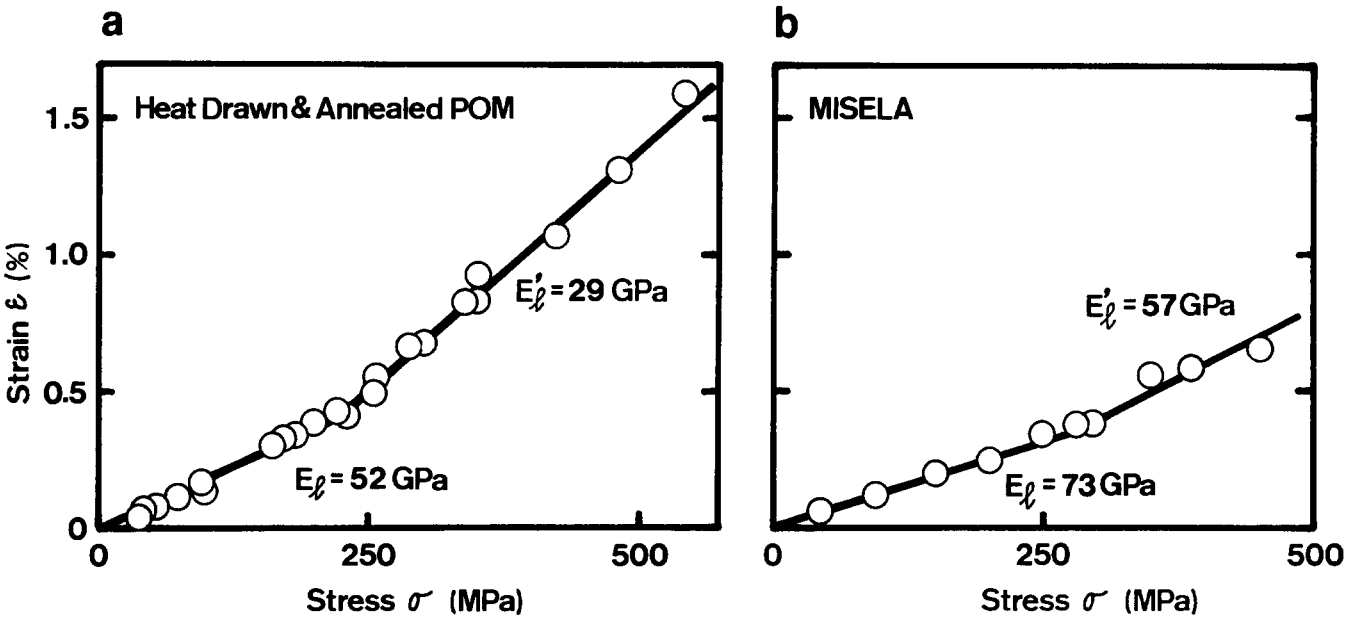

Figure 2 Stress(σ)–strain(ε) curves for the (0 0 9) plane of (a) hot-drawn and annealed POM and (b) MISELA at 25°C

force required to stretch a molecule by 1%, calculated from both E_l and the cross-sectional area (17.6 Å^2) of one molecule in a crystal lattice is 0.92×10^{-5} dyn for hot-drawn and annealed POM. These phenomena reproduce the earlier result reported by Ito *et al.*[1–4,40], where E_l, E_l', f value and stress at inflection point are 53 GPa, 36 GPa, 0.91×10^{-5} dyn and 245 MPa for drawn (150°C, 10 times) and annealed (150°C, 5 min) fibre (specific gravity = 1.410 g cm^{-3}, $X_c = 0.67$, $\Pi = 0.98$, $D_{(009)} = 175$ Å, $Y_l = 23$ GPa, fibre identity period = 17.32 Å).

Figure 3 shows the X-ray fibre photograph of hot-drawn and annealed POM under various stresses at room temperature. No transition of crystal system is observed below and above the stress corresponding to the inflection point of 230 MPa. The integral width for the (0 0 9) plane is almost constant up to 500 MPa. These suggest that the existence of the inflection point is due to the incoherent lattice vibration induced by the stress applied, but the precise reason for such behaviour is unknown at this time.

Ito *et al.*[1–4] also obtained a similar E_l value for drawn and annealed POM film (specific gravity = 1.415 g cm^{-3}, $Y_l = 5.9$ GPa). Recently, Jungnitz *et al.*[31] measured the E_l value of various kinds of POM by X-ray diffraction. They reported that the E_l value changes from sample to sample depending on its morphology, with the draw ratio and whether annealed or not. For example, the E_l value at room temperature for drawn (145°C, 9.2 times) POM film is reported to be 36 GPa from figure 2 in ref. 31, and the measured E_l value is only the apparent one. Further, Tashiro *et al.*[32] found that the stress dependence of the wavenumber of Raman and infra-red spectra change from sample to sample. They analysed these phenomena as an inhomogeneous stress distribution in the sample. However, the E_l value of hot-drawn and annealed POM is 52 GPa as shown in *Figure 2a*; furthermore, the same E_l value is obtained for drawn POM. Drawn POM, which is low drawn and not annealed, seems to correspond to the sample that is said to have a lower E_l value by Jungnitz *et al.*[31]. Therefore, whether both annealed or not and higher drawn or not, conventional POM has E_l value of 52 GPa, as previously reported[1–4,40], and this is regarded to be strong support for a homogeneous stress distribution in POM also.

Compared with the result of hot-drawn and annealed POM, E_l, E_l', f value and stress at inflection point increased to 73 GPa, 57 GPa, 1.25×10^{-5} dyn and 300 MPa for MISELA as shown in *Figure 2b*. A discrepancy arises in that the Y_l (60 GPa) value for MISELA exceeds the already reported E_l value (53 GPa)[1–4], because E_l should give us the maximum value for the specimen modulus of a polymer. However, the E_l value for MISELA is obtained as 73 GPa, which is larger than its Y_l value, and this discrepancy is dispelled. In addition, it is proper that the ratio Y_l/E_l is not unity but 0.82 for MISELA, because the crystallinity and the degree of crystal orientation do not reach limiting values.

Table 2 summarizes the observed, estimated and calculated E_l values ever reported. Observed and estimated E_l values above 100 GPa are obtained except for that obtained by X-ray diffraction. Further, calculated values scattered widely from 40 to 220 GPa depending on the assumptions and the force constants employed for the calculation.

It is very strange and interesting that the stress–strain curve and the observed E_l values differ for hot-drawn and annealed POM and MISELA as shown above, despite the fact that they are the chemically same polyoxymethylene. So we next measure the temperature dependence of E_l for these polymers from the viewpoint of the thermally activated molecular motion in the crystalline regions.

Temperature dependence of E_l of hot-drawn and annealed POM

Figure 4 shows the stress(σ)–strain(ε) curves for the (0 0 9) plane of hot-drawn and annealed POM from −150°C to +150°C. The inflection point shown at room temperature disappears below −100°C and above +110°C, and the overall σ–ε curve changes drastically with temperature. Further, the initial slope of the σ–ε curve increases gradually with increasing temperature

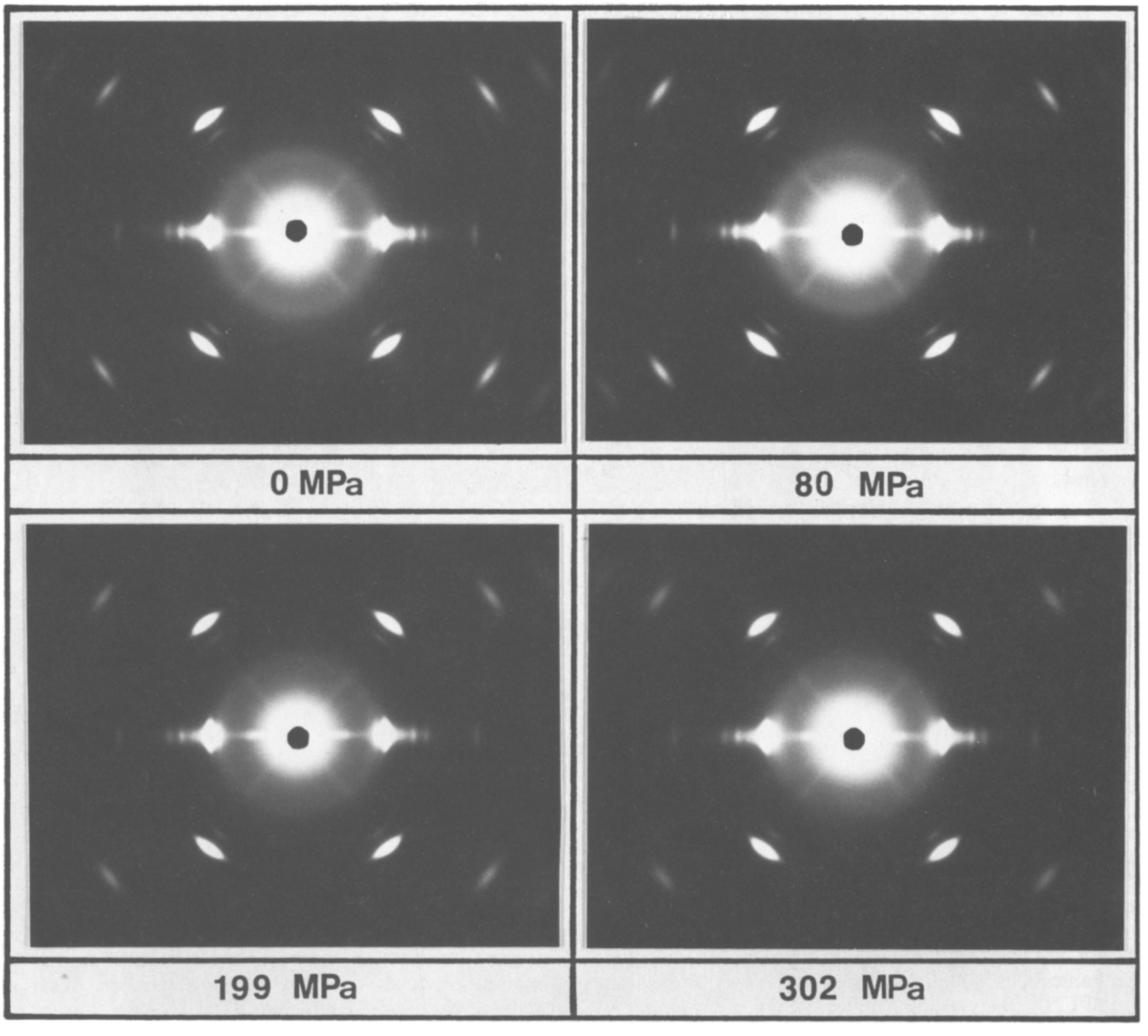

Figure 3 X-ray fibre photographs of hot-drawn and annealed POM under various stresses at 27°C

followed by abrupt increase at high temperature. This indicates the existence of a temperature dependence of the E_l of hot-drawn and annealed POM, and E_l and E_l' values are plotted against temperature in *Figure 5*.

Figure 5 shows the temperature dependence of E_l and E_l' of hot-drawn and annealed POM. The E_l value increased from 52 GPa at room temperature to 84 GPa at −150°C. With increasing temperature from −150°C, the E_l value decreased gradually, and reached a plateau value of 52 GPa up to 100°C within experimental error (±10%). After this, the E_l value decreased abruptly near 100°C and became 26 GPa above +110°C with depression of the inflection point. The same phenomena were observed for α-type poly(ethylene oxybenzoate) where the E_l value decreased abruptly from 6 to 2 GPa around 85°C with depression of the inflection point.

The open squares in *Figure 5* show the result of the temperature dependence of E_l for POM (drawn at 145°C, 20.6 times followed by annealing at 165°C, 24 h) reported by Jungnitz *et al.*[31]. Though absolute E_l values are different from ours, the tendency of the temperature-dependent behaviour of E_l agrees well with our result. On the other hand, Tashiro *et al.* reported the temperature dependence of E_l of POM above room temperature, but, in their report, the E_l value changes continuously with increasing stress and temperature without having an inflection point[32].

Figure 6 shows the X-ray fibre photographs of hot-drawn and annealed POM at various temperatures, and *Figure 7* shows the relationships between temperature and crystallite size D and lattice distortion g_{II}. From *Figure 6*, it is clear that transition of the crystal system does not take place on changing the temperature as in the case with stress. Also, D and g_{II} are unchanged from room temperature to +150°C. Here we assume that there exists paracrystalline type distortion, and use only two reflections for the determination of D and g_{II}, but the constancy of the crystallite size and distortion with temperature is maintained whether the type of distortion is first kind (e) or second type (g_{II}). These results correspond to the results of Aoki *et al.*[45], who reported that distortion of POM crystal estimated by X-ray

Table 2 Observed, estimated and calculated E_l values of POM

Methods	E_l (GPa)	Temperature (°C)	Authors	Year	Ref.
Observed					
X-ray diffraction	53	15–22	Ito *et al.*	1962	2, 3
	105	−165	Brew *et al.*	1979	27
	44	20	*ibid.*	1979	27
	51	22	Jungnitz *et al.*	1986	31
	78	−150	*ibid.*	1986	31
	47	25	Tashiro *et al.*	1988	32
	52, 73	25	This work		
	85	−150	This work		
Raman (longitudinal	189		Rabolt *et al.*	1977	33
acoustic mode)	146		Runt *et al.*	1987	34
Inelastic neutron	149		White	1976	35
scattering	164		Anderson *et al.*	1982	36
Estimated	100		Iguchi *et al.*	1982	37
	110		Takeuchi *et al.*	1984	38
	74	25	Tashiro *et al.*	1988	32
	104	−150	*ibid.*	1988	32
Calculated	150–220		Asahina *et al.*	1962	39
	72–132		Ito	1963	40
	40		Miyazawa	1965	41
	153		Piseri *et al.*	1968	42
	95		Sugeta *et al.*	1970	43
	109		Tashiro *et al.*	1988	32
	64		Sorensen *et al.*	1988	44

diffraction is mainly due to thermal vibration. As a result, the abrupt decrement of E_l above +100°C is considered not to be due to partial melting of crystallites, nor the increment of distortion, nor the transition of crystal system induced by temperature changes. In addition, mechanical crystalline dispersion is reported to begin at +100°C[46]. These results indicate that the mobility of chain molecules in the crystalline regions increased abruptly above +100°C. E_l' began to appear above −100°C, and decreased discontinuously around −30°C, after which E_l and E_l' coincide with each other above 110°C. This implies that the deformation mechanism of the POM molecule in a upper stress region at room temperature apparently agrees well with that in an initial stress region at high temperature. Further discussion will be needed on this point.

Specimen modulus Y_l of 27 GPa at room temperature decreased gradually with increasing temperature and reached 4.4 GPa at 100°C, while E_l is constant in this temperature range. Hence, the decrement of Y_l can be attributed to the decrement of the elastic modulus E_a of amorphous regions. If the crystalline regions are considered to be parallel with the amorphous regions, the decrement of E_a will lead to the concentration of stress on the crystalline regions, and therefore E_l should apparently decrease with increasing temperature. However, in our measurement, E_l did not decrease with increasing temperature up to +100°C despite the fact that E_a decreased. Then, it is reasonable to conclude that our homogeneous stress distribution model is proved.

We have already measured the temperature dependence of E_l of various polymers[16–26]. It has been found that E_l decreased above a certain temperature except for poly(ethylene terephthalate) (PET) and isotactic poly(4-methyl-1-pentene) (P4M1P). This characteristic temperature is in accordance with the temperature range where thermal contraction of a polymer chain in the crystalline regions changed. In contrast with these cases, E_l values remain unchanged until the axial thermal expansion coefficient α_c is constant, such as for PET and P4M1P. Thus, we next measure the thermal expansion behaviour of crystal lattice for hot-drawn and annealed POM.

Figure 8 shows the relationship between temperature and lattice spacing for the (0 0 9) plane of hot-drawn and annealed POM. Measurement was performed in a cooling process. White *et al.* investigated the axial thermal expansion of polymerized trioxane, and found that the thermal expansion coefficient is negative at low temperature, but positive above 100 K[47]. However, the (0 0 9) spacing of hot-drawn and annealed POM contracts with increasing temperature. This means that α_c is always negative in the temperature range studied. Recently, the same result was obtained by Choy *et al.*[48]. Further, α_c changed discontinuously at −20 and +100°C. These phenomena are also observed for the temperature dependence of the lattice spacing for the (0 0 18) plane. These results show that the mobility of chain molecules along the chain axis changed around both −20 and +100°C. Comparing the temperature dependence of E_l with that of (0 0 9) spacing, they resemble each other. That is, with increasing temperature, E_l decreases gradually and reached a constant value of 52 GPa at −20°C, where α_c changed. Further, the abrupt decrement of E_l corresponds to the decrease of α_c above +100°C. Accordingly,

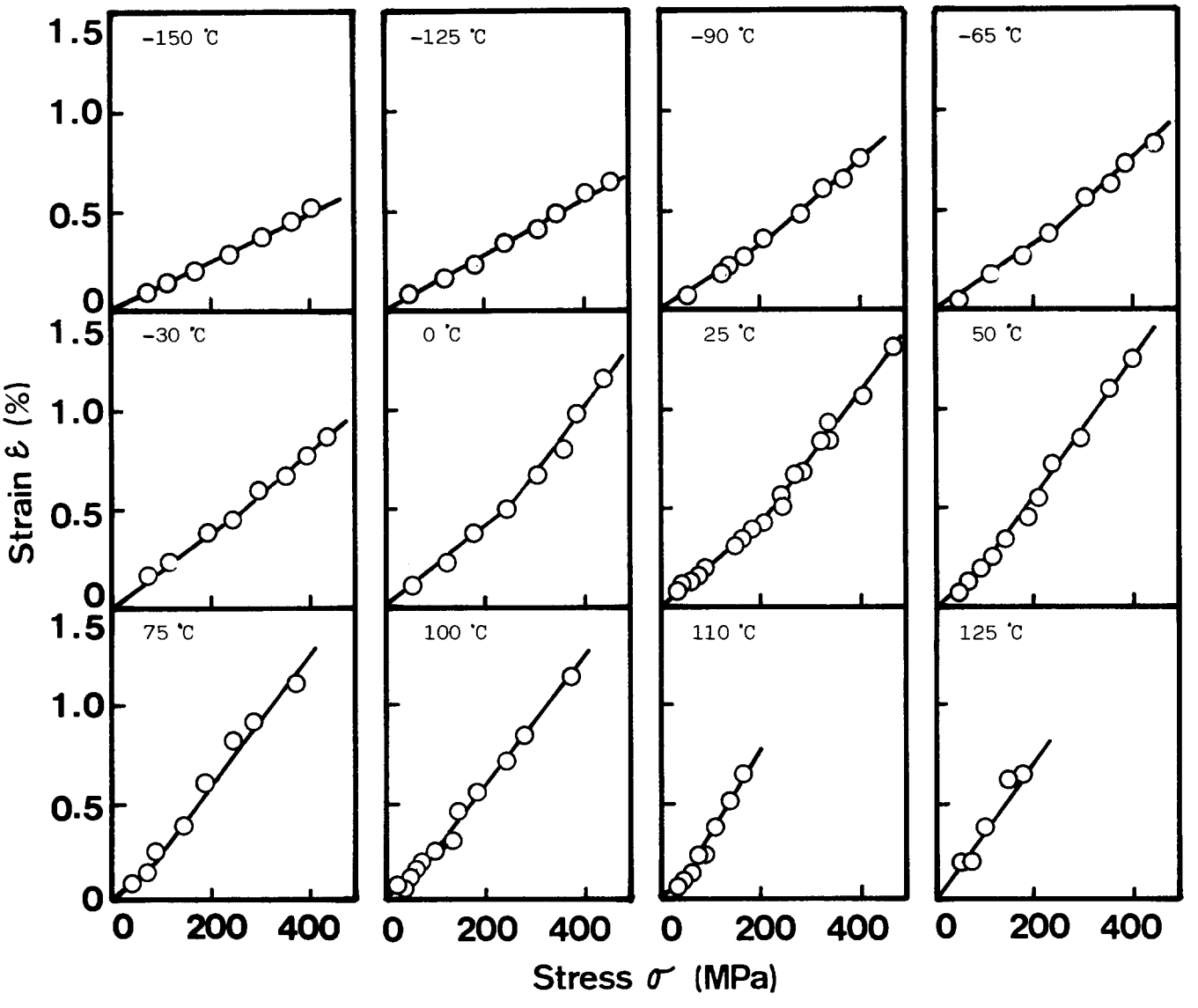

Figure 4 Stress(σ)–strain(ε) curves for the (009) plane of hot-drawn and annealed POM at various temperatures

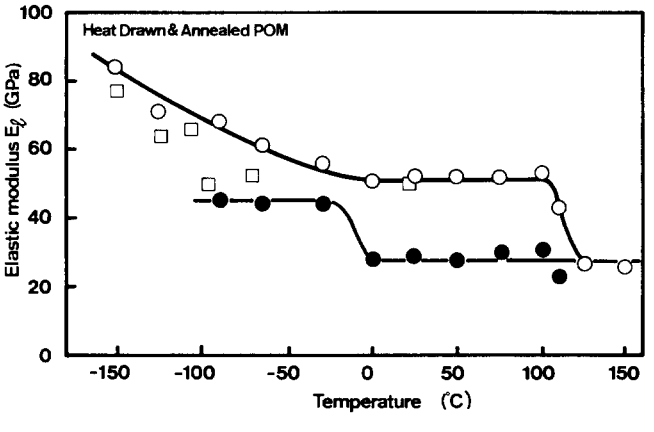

Figure 5 Effect of temperature on the elastic modulus E_l and E_l' of hot-drawn and annealed POM. Symbol □ indicates the E_l value obtained by Jungnitz *et al.*[31]

the change of the mobility of chain molecules in the crystaline regions, i.e. incoherent thermal vibration of the crystal lattice, is considered to cause the temperature dependence of E_l for hot-drawn and annealed POM.

Temperature dependence of E_l of MISELA

Figure 9 shows the stress(σ)–strain(ε) curves for the (009) plane of MISELA at various temperatures. The σ–ε curves below −30°C and above +110°C can be expressed with a straight line through zero. An inflection point of σ–ε curves appears between 0 and +100°C. Lattice extensions are also reversible at each temperature.

Figure 10 shows the relationships between temperature and E_l and E_l' of MISELA. E_l is 86 GPa at −150°C, which agrees well with the E_l value of hot-drawn and annealed POM. With increasing temperature, E_l gradually decreased and reached 73 GPa above −60°C. This is in contrast with the case of hot-drawn and annealed POM, in which E_l reached 52 GPa above 0°C. Furthermore, E_l abruptly decreased to become 52 GPa above +110°C, with vanishing of the inflection point of σ–ε curves. The E_l value seems to coincide with the E_l' value above 110°C.

Figure 11 shows the comparison of the temperature dependence of E_l with that of dynamic modulus and tan δ of MISELA ($\lambda = 33$) at 3.5 Hz reported by Konaka *et al.*[49]. They reported the specimen modulus Y_l of MISELA to be 77 GPa at −150°C, 58 GPa at room temperature and 48 GPa at 100°C. These values correspond to 90%,

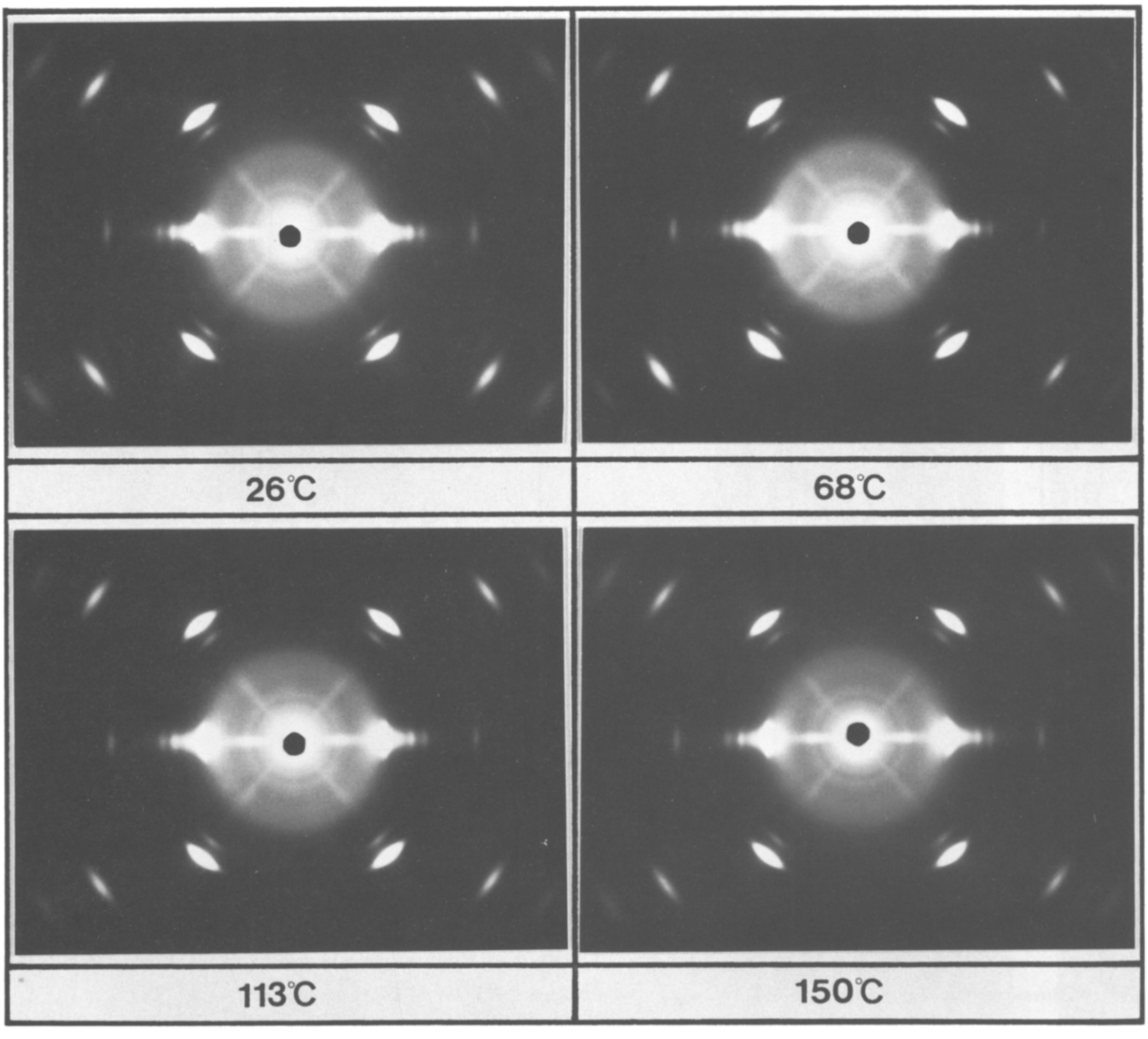

Figure 6 X-ray fibre photographs of hot-drawn and annealed POM at various temperatures

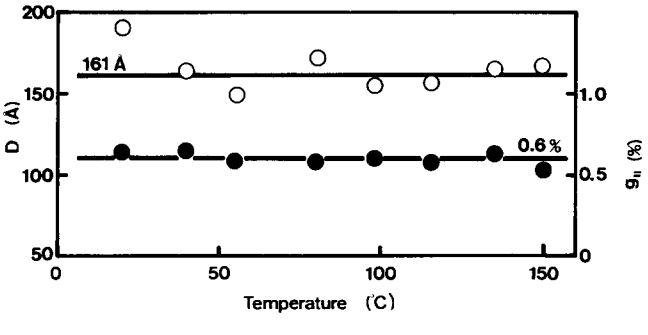

Figure 7 Relationships between temperature and the crystallite size D and the lattice distortion g_{II} in the direction of chain axis for hot-drawn and annealed POM

80% and 67% of E_l respectively. Although dynamic modulus does not necessarily correspond directly to the E_l value, the relation $E_l > Y_l$ is always satisfied in the temperature range studied. The tendencies of the temperature dependences resemble each other below −60°C.

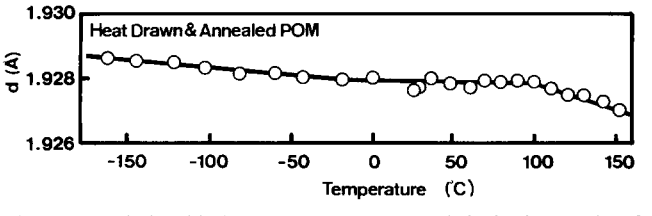

Figure 8 Relationship between temperature and the lattice spacing d for the (009) plane of hot-drawn and annealed POM

This shows that specimen modulus and its temperature dependence is almost determined by E_l in this temperature range. Further, the decrement of E_l at 100°C corresponds to the rise in tan δ, which is considered to be associated with crystalline dispersion. Though MISELA and hot-drawn and annealed POM are chemically the same polyoxymethylene, the absolute values of E_l and its temperature-dependent behaviour are much different from each other. So, next, we measure the thermal expansion behaviour of the crystal lattice for MISELA, too.

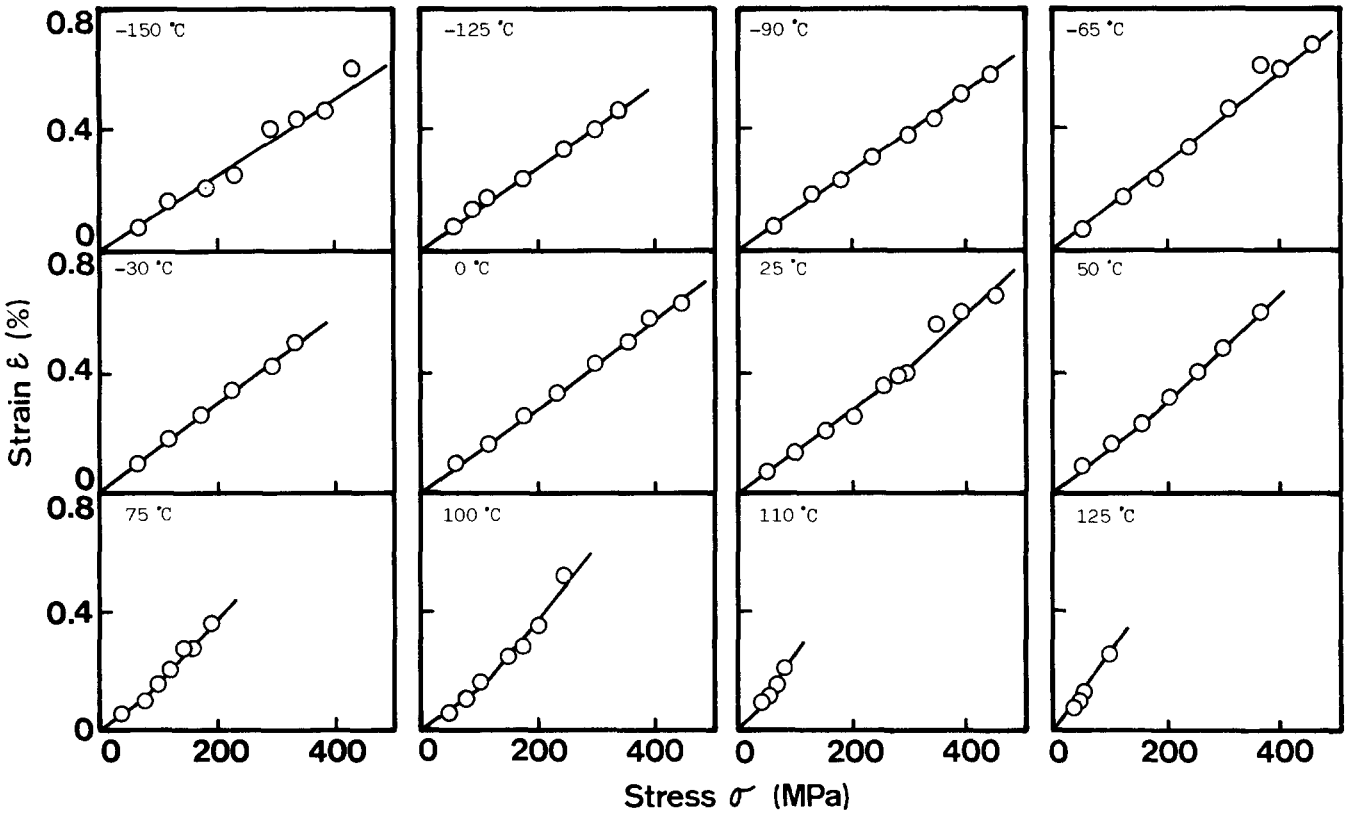

Figure 9 Stress(σ)–strain(ε) curves for the (009) plane of MISELA at various temperatures

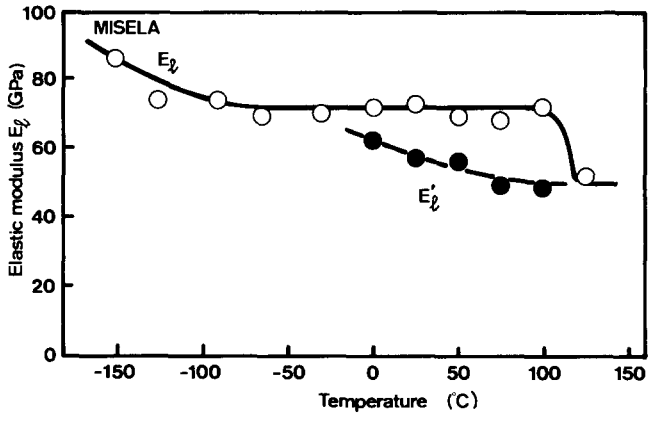

Figure 10 Effect of temperature on the elastic modulus E_l and E_l' of MISELA

Figure 12 shows the relationship between temperature and lattice spacing for the (009) plane of MISELA. With increasing temperature, chain molecules of MISELA contract with inflection points around -60 and $+100$°C. These temperature ranges where α_c changes agree well with the temperature ranges where E_l changes as shown in *Figure 10*. Therefore, the temperature dependence of E_l of MISELA is also due to the change of mobility of chain molecules in the crystalline regions.

From n.m.r., Chiba *et al.*[50] and Shibata *et al.*[51] observed that large-amplitude oscillations in the crystalline regions occur even at low temperature and the amplitude increases with increasing temperature. This oscillation is also reported to be attributed not only to the rotational oscillation around the helix axis, but also to the longitudinal oscillation along the helix axis, which

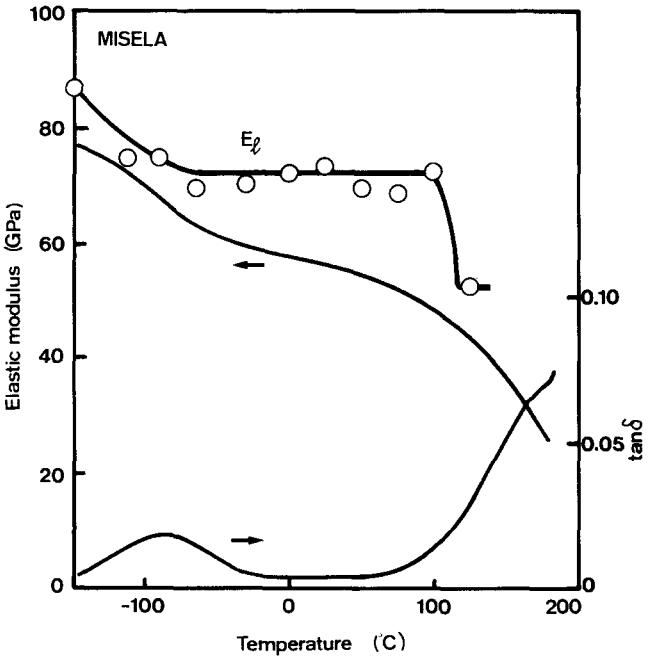

Figure 11 Comparison of temperature dependence of E_l with that of dynamic modulus and tan δ of MISELA at 3.5 Hz[49]

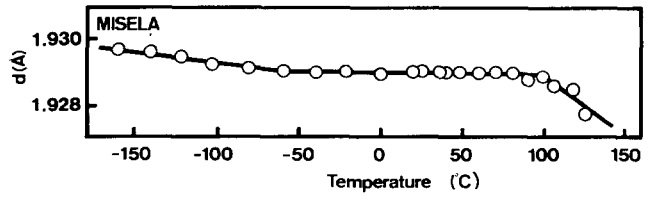

Figure 12 Relationship between temperature and lattice spacing for the (009) plane of MISELA

Table 3 Thermal expansion coefficient α_c ($10^{-6}K^{-1}$) for the (009) plane of various POM

Hot-drawn and annealed POM		MISELA	
	−2.4		−3.3
−20°C		−60°C	
	−0.45		−0.24
100°C		100°C	
	−7.8		−18.2

involves the change of internal rotation angle in the crystalline regions. The latter motion is expected to influence the E_l value, and this is considered to cause the decrease of E_l as shown in *Figures 5* and *10*. Anyhow, the elastic modulus E_l parallel to the chain axis is temperature-dependent and there exists an inflection point of thermal contraction behaviour for the crystal lattice of POM. These results show that thermally excited molecular motion involves longitudinal molecular motion along the chain axis.

Table 3 shows the thermal expansion coefficient α_c of hot-drawn and annealed POM and MISELA. The temperature regions where α_c changed are different for each POM, and the large values of α_c do not lead to small E_l values. Molecular motion at room temperature is considered to be more enhanced than that at low temperature, though α_c at room temperature is smaller than α_c at low temperature for both samples. Thus, the absolute value of α_c does not always correspond to the intensity of molecular motion. However, the discontinuous change of α_c indicates the change of patterns of molecular motion, which lead to the decrement of E_l as was shown for many polymers. The difference of the value of α_c for each POM also means that there exists some difference in molecular motion.

Consequently, the mobility of chain molecules, i.e. incoherent thermal vibration, differs from hot-drawn and annealed POM to MISELA, and this causes the difference in temperature dependence of E_l for the two kinds of POMs. Further, the discrepancy of E_l values for these samples at room temperature is in fact not because of the inhomogeneous stress distribution, but because of the difference in the mobility of chain molecules in the crystalline regions at room temperature.

ACKNOWLEDGEMENT

This work was partially supported by a Grant-in-Aid for Science Research from the Ministry of Education, Science and Culture of Japan.

REFERENCES

1 Sakurada, I., Nukushina, Y. and Ito, T. *J. Polym. Sci.* 1962, **57**, 651
2 Sakurada, I., Ito, T. and Nakamae, K. *Makromol. Chem.* 1964, **75**, 1
3 Sakurada, I., Ito, T. and Nakamae, K. *J. Polym. Sci. C.* 1966, **15**, 75
4 Sakurada, I. and Kaji, K. *J. Polym. Sci.* (*C*) 1970, **31**, 57
5 Sakurada, I. and Kaji, K. *Makromol. Chem., Suppl.* 1975, **1**, 599
6 Nakamae, K., Yokoyama, F., Nishino, T., Yoshikawa, M. and Matsumoto, T. *J. Macromol. Sci.-Phys.* (*B*) 1983, **22**, 591
7 Nakamae, K., Nishino, T., Shimizu, Y. and Matsumoto, T. *Polym. J.* 1987, **19**, 451
8 Uchida, T. and Tadokoro, H. *J. Polym. Sci.* (*A-2*) 1967, **5**, 63
9 Ciferri, A. and Ward, I. M. (Eds.), 'Ultra High Modulus Polymers', Applied Science, Barking, Essex, 1979
10 Slutsker, A. I., Gromov, A. E. and Pshezhetskii, V. S. *Soviet Phys.-Solid State* 1964, **6**, 362
11 Clark, E. S. and Scott, L. S. *Polym. Eng. Sci.* 1974, **14**, 682
12 Brew, B. and Ward, I. M. *Polymer* 1978, **19**, 1338
13 Coates, P. D. and Ward, I. M. *J. Polym. Sci., Polym. Phys. Edn.* 1978, **16**, 2031
14 Komatsu, T., Enoki, S. and Aoshima, A. *Polym. Prepr. Jpn.* 1986, **34**, 3712
15 Nakagawa, K., Konaka, T. and Yamakawa, S. *Polymer* 1985, **26**, 84
16 Nishino, T., Yokoyama, F., Nakamae, K. and Matsumoto, T. *Kobunshi Ronbunshu* 1983, **40**, 357
17 Nakamae, K., Nishino, T., Hata, K. and Matsumoto, T. *Kobunshi Ronbunshu* 1985, **42**, 241
18 Nakamae, K., Nishino, T., Hata, K. and Matsumoto, T. *Kobunshi Ronbunshu* 1985, **42**, 361
19 Nishino, T., Hata, K., Nakamae, K. and Matsumoto, T. *Rep. Poval Committee* 1985, **86**, 8
20 Nakamae, K., Nishino, T., Hata, K. and Matsumoto, T. *Kobunshi Ronbunshu* 1986, **43**, 133
21 Nakamae, K., Nishino, T., Shimizu, Y., Hata, K. and Matsumoto, T. *Kobunshi Ronbunshu* 1986, **43**, 499
22 Nakamae, K., Nishino, T., Hata, K., Ohkubo, H. and Matsumoto, T. Prepr. 2nd SPSJ Int. Polym. Conf., 1986, p. 98
23 Nakamae, K., Nishino, T., Hata, K. and Matsumoto, T. *Kobunshi Ronbunshu* 1987, **44**, 421
24 Nishino, T., Sugihashi, T. and Nakamae, K. *Kobunshi Ronbunshu* 1988, **45**, 979
25 Nakamae, K., Nishino, T., Yokoyama, F. and Matsumoto, T. *J. Macromol. Sci.-Phys.* (*B*) 1988, **27**(4), 407
26 Nakamae, K., Nishino, T. and Takagi, S. Prepr. 34th Kobe Annual Meeting Soc. Polym. Sci. Jpn. 1988, p. 83
27 Brew, B., Clements, J., Davies, G. R., Jakeways, R. and Ward, I. M. *J. Polym. Sci., Polym. Phys. Edn.* 1979, **17**, 351
28 Korenaga, T., Hamada, F. and Nakajima, A. *Polym. J.* 1972, **3**, 21
29 Jones, F. W. *Proc. R. Soc.* (*A*) 1938, **166**, 16
30 Hosemann, R. and Wilke, W. *Makromol. Chem.* 1968, **118**, 230
31 Jungnitz, S., Jakeways, R. and Ward, I. M. *Polymer* 1986, **27**, 1651
32 Tashiro, K., Wu, G. and Kobayashi, K. *Polymer* 1988, **29**, 1768; Tashiro, K. *Sen'i Gakkai Prepr.* 1988, **1988**, S-96
33 Rabolt, J. F. and Fanconi, B. *J. Polym. Sci., Polym. Lett. Edn.* 1977, **15**, 121
34 Runt, J., Wagner, R. F. and Zimmer, M. *Macromolecules* 1987, **20**, 2531
35 White, J. W. 'Structural Studies of Macromolecules by Spectroscopic Methods', (Ed. K. J. Ivin), Wiley, London, 1976, p. 41
36 Anderson, M. R., Harryman, M. B. M., Steinman, D. K. and White, J. W. *Polymer* 1982, **23**, 569
37 Iguchi, M., Suehiro, T., Watanabe, Y., Nishi, Y. and Uryu, M. *J. Mater. Sci.* 1982, **17**, 1632
38 Takeuchi, Y., Yamamoto, F. and Nakagawa, K. *J. Polym. Sci., Polym. Lett. Edn.* 1984, **22**, 159
39 Asahina, M. and Enomoto, S. *J. Polym. Sci.* 1962, **59**, 101; *ibid.* 1962, **59**, 113
40 Ito, T. Doctoral Thesis, Kyoto University, 1963
41 Miyazawa, T. *Rep. Progr. Polym. Phys. Jpn.* 1965, **8**, 47
42 Piseri, L. and Zerbi, G. *J. Chem. Phys.* 1968, **48**, 3561
43 Sugeta, H. and Miyazawa, T. *Polym. J.* 1970, **1**, 226
44 Sorensen, R. A., Liau, W. B., Kesner, L. and Boyd, R. H. *Macromolecules* 1988, **21**, 200
45 Aoki, Y., Chiba, A. and Kaneko, M. *Rep. Progr. Polym. Phys. Jpn.* 1969, **12**, 187
46 Takayanagi, M., Minami, S., Neki, K. and Nagai, A. *J. Soc. Mater. Sci. Jpn* 1965, **14**, 343
47 White, G. K., Smith, T. F. and Birch, J. A. *J. Chem. Phys.* 1976, **65**, 554
48 Choy, C. L. and Nakafuku, C. *J. Polym. Sci.* (*B*) *Polym. Phys. Edn.* 1988, **26**, 921
49 Konaka, T., Nakagawa, K. and Yamakawa, S. *Polymer* 1985, **26**, 462
50 Chiba, A., Hasegawa, A., Hikichi, K. and Furuichi, J. *J. Phys. Soc. Jpn* 1966, **21**, 1777
51 Shibata, T. and Iwayanagi, S. *Polym. J.* 1978, **10**, 599